

Parton densities and structure functions beyond the next-to-leading order

W.L. van Neerven and A. Vogt ^{a*}

^aInstituut-Lorentz, University of Leiden, P.O. Box 9506, 2300 RA Leiden, The Netherlands

We discuss recent results on the evolution of unpolarized parton densities and structure functions in massless perturbative QCD. Present partial results on the next-to-next-to-leading order (NNLO) evolution kernels prove sufficient for reliable calculations at not too small values of the Bjorken variable, $x > 10^{-3}$. One order more can be taken into account at $x \geq 0.2$. Inclusion of these terms considerably reduces the main theoretical uncertainties of determinations of α_s (to about 1% at the Z -mass) and the parton densities from structure functions.

1. Introduction

Structure functions in deep-inelastic scattering (DIS) are among the quantities best suited for measuring the strong coupling constant α_s . They also form the backbone of our knowledge of the proton's parton densities, indispensable for analyses of hard scattering processes at proton-(anti-)proton colliders like TEVATRON and the LHC. During the past two decades DIS experiments have proceeded towards high accuracy and a greatly extended kinematic coverage [1].

To make full use of these results requires transcending the standard next-to-leading order (NLO) formalism [2]. Indeed besides the QCD β -functions to even NNNLO [3,4], the NNLO (2-loop) coefficient functions for DIS have been calculated some time ago [5,6]. However, only partial results have been obtained so far for the corresponding 3-loop splitting functions [7–13]. The derivation of the full results is under way [14].

In [15,16] we have derived approximate expressions for the 3-loop $\overline{\text{MS}}$ splitting functions which are sufficient for reliable NNLO analyses down to $x \simeq 10^{-3}$. These functions turn out to be much less important than the 2-loop coefficient functions at $x \geq 10^{-2}$. Thus it is possible, based on partial results [7,8,17,18] on the 3-loop coefficient functions, to proceed to NNNLO at large x [19], especially for the non-singlet case most important for extractions of α_s from DIS.

*Work supported by the EC TMR program under contract No. FMRX-CT98-0194. Presented by A. Vogt at 'Loops and Legs in QFT', Bastei (Germany), April 2000.

2. Parton densities: formalism

It is convenient to work with the flavour non-singlet (NS) and singlet (S) combinations of the (anti-)quark and gluon densities, q_i , \bar{q}_i and g :

$$\begin{aligned} q_{\text{NS}}^{\pm} &= q_i \pm \bar{q}_i - (q_k \pm \bar{q}_k) \\ q_{\text{NS}}^V &= \sum_{r=1}^{N_f} (q_r - \bar{q}_r) \\ q_S &= \begin{pmatrix} \Sigma \\ g \end{pmatrix}, \quad \Sigma = \sum_{r=1}^{N_f} (q_r + \bar{q}_r). \end{aligned} \quad (1)$$

Here N_f is the number of effectively massless flavours. As in (1) we often suppress the dependence on the momentum fraction x and the renormalization and factorization scales, μ_r and μ_f .

Using (1) the evolution equations are decomposed into $2N_f - 1$ scalar (NS) equations and the 2×2 singlet system, all schematically written as

$$\frac{d}{d \ln \mu_f^2} q = \mathcal{P} \otimes q \equiv \int_x^1 \frac{dy}{y} \mathcal{P}(y) q\left(\frac{x}{y}\right). \quad (2)$$

At $\mu_r = \mu_f$ the expansion of the splitting functions \mathcal{P} up to NNLO is given by

$$\mathcal{P} \simeq a_s P^{(0)}(x) + a_s^2 P^{(1)}(x) + a_s^3 P^{(2)}(x). \quad (3)$$

Our choice of the expansion parameter reads

$$a_s \equiv \alpha_s / 4\pi. \quad (4)$$

The expression for $\mu_r \neq \mu_f$ is obtained from (3) by inserting the expansion of $a_s(\mu_f^2)$ in terms of $a_s(\mu_r^2)$ and $L_R = \ln(\mu_f^2/\mu_r^2)$. Large logarithms in \mathcal{P} are avoided by choosing $\mu_r = O(\mu_f)$.

3. Splitting functions

The functions $P^{(0)}$ and $P^{(1)}$ in (3) are known [2]. The current information on $P_{\text{NS}}^{(2)\pm}(x)$ comprises

- the first five even-integer moments of $P_{\text{NS}}^{(2)+}$ given by $P_{\text{NS}}^{(2)+}(N) = \int_0^1 dx x^{N-1} P_{\text{NS}}^{(2)+}(x)$ [7,8], and the first moment ($N=1$) of $P_{\text{NS}}^{(2)-}$,
- the complete N_f^2 contribution [9],
- the leading small- x terms $\propto \ln^4 x$ [10].

The difference of $P_{\text{NS}}^{(2)-}$ and $P_{\text{NS}}^{(2)+}$ is expected to be negligible at large x . It has been conjectured that the leading large- x terms are $\propto 1/[1-x]_+$ [20].

The following partial results have been derived so far for the singlet splitting functions $P_{ij}^{(2)}(x)$:

- $P_{ij}^{(2)}(N)$ for $N = 2, 4, 6$ and 8 [8],
- the $C_A N_f^2$ contribution to $P_{gg}^{(2)}(x)$ [11],
- the leading small- x terms $\propto (1/x) \ln x$ of $P_{qq}^{(2)}$, $P_{qg}^{(2)}$ [12] and $P_{gg}^{(2)}$ [13], see also [21].

The $1/[1-x]_+$ terms of $P_{gg}^{(2)}$ and $P_{qq}^{(2)}$ are expected to be related by a factor $C_A/C_F = 9/4$.

We have derived approximate expressions for $P_{\text{NS}}^{(2)\pm}(x)$ and $P_{ij}^{(2)}(x)$ from these constraints. After decomposing the functions into

$$P^{(2)} = P_0^{(2)} + N_f P_1^{(2)} + N_f^2 P_2^{(2)}, \quad (5)$$

we employ the ansatz (cf. [8])

$$P_m^{(2)}(x) = \sum_{n=1}^{n_m} A_n f_n(x) + f_e(x). \quad (6)$$

The basis functions f_n are build up of $1/[1-x]_+$, $\delta(1-x)$ and of powers of $\ln(1-x)$, x , and $\ln x$. The coefficients A_n are determined from the $n_m=5$ ($n_m=4$) linear equations provided by the non-singlet (singlet) moments of [7,8] after taking into account the other constraints collected in f_e in (6). The remaining uncertainties are estimated by ‘reasonably’ varying the choice of the basis functions f_n , typically considering some 20 to 40 trial functions. Finally two approximations

spanning the error band are selected, except for the highest unknown N_f -contributions in (5) for which one central representative is sufficient.

This procedure is briefly illustrated in Fig. 1 for the $N_f = 0$ part of $P_{\text{NS}}^{(2)+}(x)$. The upper plot shows 24 trial functions. The approximations A and B emphasized in the plot have been selected, after considering also the convolution with a typical input shape shown for these two functions in the lower plot. As can be inferred from Fig. 1, the presence of the convolution in (2) considerably increases the effective accuracy of our approximations illustrated in Figs. 1 and 2: The convolutions smoothen out the oscillating large- x differences between different approximations to a large extent. They also partly compensate the large small- x uncertainties of $P^{(2)}$ present despite the $x \rightarrow 0$ constraints of [10,12,13].

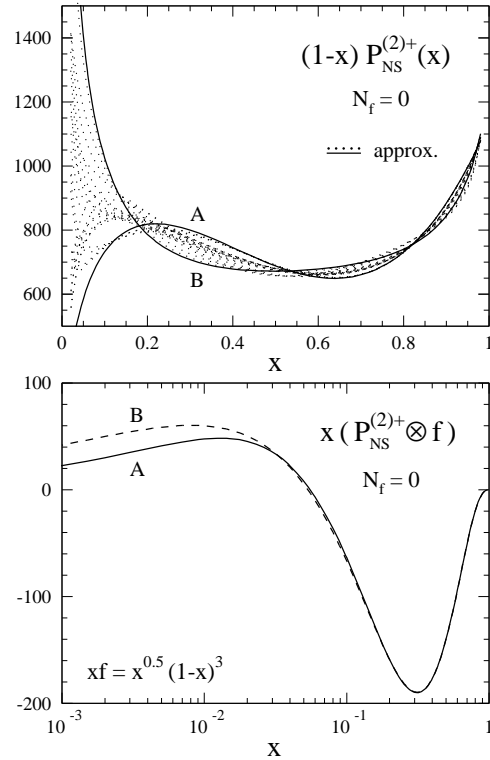


Figure 1. Top: $P_{\text{NS}}^{(2)+}$ for $N_f=0$, as obtained from the results of [7,8,10] by means of (6). Bottom: Convolutions of the selected approximations A and B with a typical non-singlet input shape.

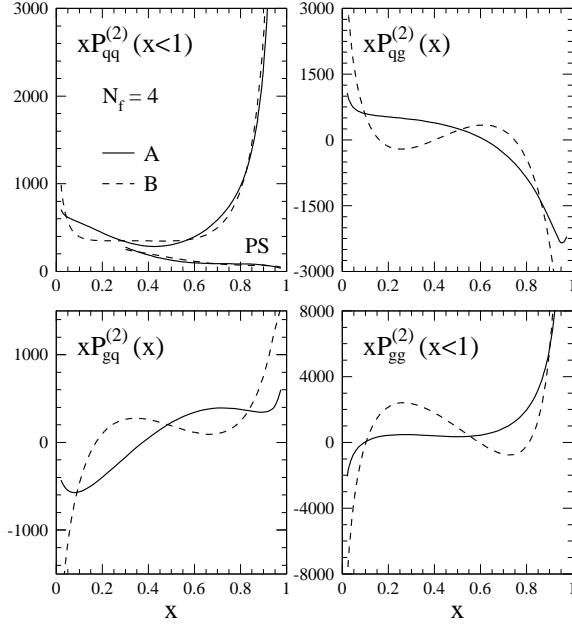


Figure 2. The approximations selected for $P_{ij}^{(2)}$ for $N_f = 4$. The pure singlet (PS) contribution $P_{qq}^{(2)} - P_{NS}^{(2)+}$ is also shown at $x \geq 0.3$.

4. Parton densities: results

We illustrate the impact of the NNLO terms on the parton evolution by the derivatives $\dot{q} \equiv d \ln q / d \ln \mu_f^2$, $q = q_{NS}^+$, Σ , g , at a reference scale

$$\mu_f^2 = \mu_{f,0}^2 \approx 30 \text{ GeV}^2 \quad (7)$$

corresponding to $\alpha_s(\mu_r^2 = \mu_{f,0}^2) = 0.2$. The input densities adopted for the non-singlet case read

$$xq_{NS}^+ = x^{0.5}(1-x)^3. \quad (8)$$

For the singlet distributions we employ

$$\begin{aligned} x\Sigma(\mu_{f,0}^2) &= 0.6 x^{-0.3} (1-x)^{3.5} (1+5x^{0.8}) \\ xg(x, \mu_{f,0}^2) &= 1.0 x^{-0.37} (1-x)^5. \end{aligned} \quad (9)$$

The dependence of the results on the renormalization scale is presented via

$$\Delta \dot{q} \equiv \frac{\max \dot{q} - \min \dot{q}}{2 |\text{average } \dot{q}|}, \quad (10)$$

where μ_r is varied over the conventional interval

$$1/4 \mu_f^2 \leq \mu_r^2 \leq 4 \mu_f^2. \quad (11)$$

The NNLO effects on the derivatives \dot{q} and the NLO and NNLO scale uncertainties $\Delta \dot{q}$ are shown in Figs. 3 and 4. The present inaccuracies of the NNLO results caused by the uncertainties remaining for the functions $P^{(2)}$ are represented by the bands spanned by the NNLO_A and NNLO_B curves. The central results $\frac{1}{2}(\text{NNLO}_A + \text{NNLO}_B)$ are not shown separately.

The uncertainties of the NNLO derivatives \dot{q} due to the approximations for $P^{(2)}$ are entirely negligible for $x \gtrsim 0.1$. They increase towards very small values of x , but do not exceed $\pm 2\%$ above $x \simeq 10^{-3}$ (or a few times this number for scales μ_f much smaller than (7)). Given the small size of the NNLO corrections and the weak μ_r -dependence remaining at NNLO, one can safely estimate that contributions beyond NNLO affect the parton evolution, for $\alpha_s \lesssim 0.2$, by less than 1% at large x and 2% down to $x \simeq 10^{-3}$.

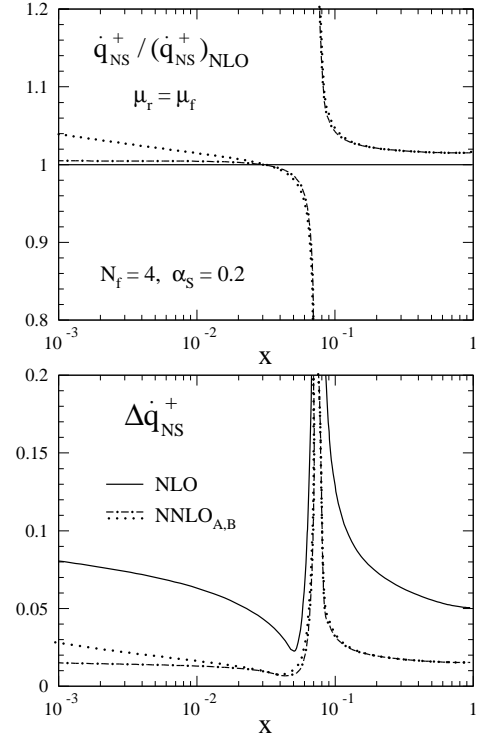


Figure 3. Top: The NNLO corrections for $\dot{q}_{NS}^+ \equiv d \ln q_{NS}^+ / d \ln \mu_f^2$ at $\mu_f = \mu_{f,0}$ for the input (8). Bottom: The relative μ_r -uncertainty of the NLO and NNLO results for \dot{q}_{NS}^+ using (10) and (11).

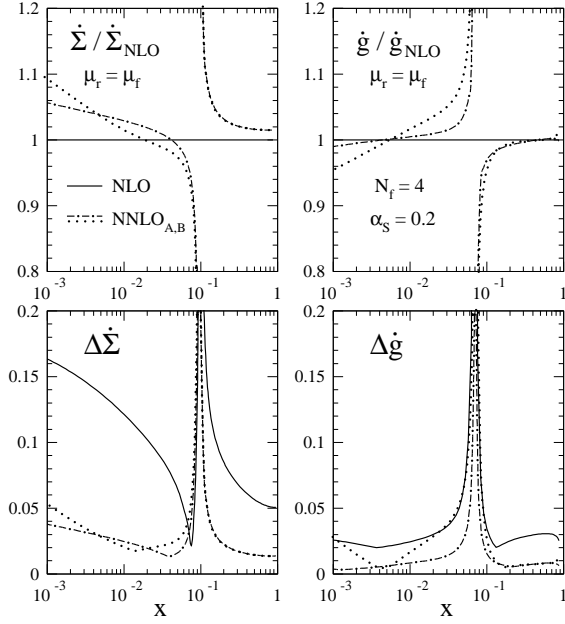


Figure 4. As Figure 3, but for the singlet quark and gluon densities Σ and g given in (8) and (9). The spikes close to $x=0.1$ in both figures are due to zeros of the respective denominators.

5. Structure functions: formalism

The unpolarized non-singlet ($a = 1, 2, 3$) and singlet ($a = 1, 2$) structure functions F_a are obtained by convoluting the solutions $q(\mu_f^2, \mu_r^2)$ of (2) with the corresponding coefficient functions,

$$\eta_a F_a(x, Q^2) = [\mathcal{C}_a(a_s, L_M, L_R) \otimes q](x) . \quad (12)$$

For $L_M = \ln(Q^2/\mu_f^2) \neq 0$, but $\mu_r = \mu_f$ ($L_R = 0$):

$$\mathcal{C}_a = c_a^{(0)}(x) + \sum_{l=1} a_s^l \left\{ c_a^{(l)}(x) + \sum_{m=1}^l c_a^{(l,m)}(x) L_M^m \right\} \quad (13)$$

with $\mathcal{C}_a = (\mathcal{C}_{a,q}, \mathcal{C}_{a,g})$ in the singlet case. The coefficients η_a in (13) include the charge factors so that $c_{a,\text{NS}}^{(0)} = c_{a,q}^{(0)} = \delta(1-x)$, whereas, of course, $c_{a,g}^{(0)} = 0$. The contributions $c_a^{(l,m)}$ fixed by renormalization-group constraints are build up of the $c_a^{(k)}$ and the splitting functions $P^{(k)}$ up to $k = l-1$. The generalization of (13) to $\mu_r \neq \mu_f$ proceeds as indicated below (4).

The scaling violations of the non-singlet structure functions can be conveniently expressed in terms of these structure functions themselves (thereby removing any dependence on μ_f), viz

$$\frac{d}{d \ln Q^2} F_{a,\text{NS}} = \mathcal{K}_{a,\text{NS}} \otimes F_{a,\text{NS}} . \quad (14)$$

The kernels $\mathcal{K}_{a,\text{NS}}$ are derived by differentiating (12) with respect to $\ln Q^2$ and then eliminating the quark densities using the same equation.

6. Coefficient functions

Besides the functions $c_a^{(1)}$ in (13), see [2], also the NNLO contribution $c_a^{(2)}$ are known [5,6]. Those expressions are rather lengthy and involve higher transcendental functions. We have thus provided compact approximations which are sufficiently accurate for any foreseeable application.

As illustrated below (Fig. 6), the impact of the functions $c_a^{(2)}$ (especially of the quark coefficient functions which contain large soft-gluon emission terms) is much larger than that of the splitting functions $P^{(2)}$ at $x > 10^{-2}$. The same situation is expected for the NNNLO quantities $c_a^{(3)}$ and $P^{(3)}$. Hence a good approximation to the NNNLO at large x can be obtained by just retaining the $c_a^{(3)}$.

The current information on the $c_a^{(3)}$ comprises

- the first five even-integer moments of $c_{2,\text{NS}}^{(3)+}$ and the first four of $c_{2,q}^{(3)}$ and $c_{2,g}^{(3)}$ [7,8],
- the four leading large- x terms $\propto \ln^k(1-x)/[1-x]_+$, $k = 2, \dots, 5$ of $c_{a,\text{NS}}^{(3)}$ and $c_{a,q}^{(3)}$ [8,18], fixed by the results of [17], together with those of [5] for $k = 2$.

For $c_{2,\text{NS}}^{(3)-}$ only the first moment ($= 0$) is known from the Adler sum rule. However, the results on $c_{2,\text{NS}}^{(2)\pm}$ indicate that the difference $c_{2,\text{NS}}^{(3)-} - c_{2,\text{NS}}^{(3)+}$ has a negligibly small effect. Results for the lowest moments of $c_3^{(3)}$ will become available soon [22].

Focusing on the non-singlet case most relevant for α_s -determinations from structure functions, we have employed the above information to derive approximations of $c_{2,\text{NS}}^{(3)}(x)$ [19]. The impact of their residual uncertainties is small for $x \geq 0.2$.

7. Structure functions: results

We illustrate the effect of the NNLO (and NNNLO) terms on the structure functions at

$$Q^2 \approx 30 \text{ GeV}^2. \quad (15)$$

In (14) we employ the non-singlet input shape

$$F_{2,\text{NS}}^+(x, Q^2) = x^{0.5}(1-x)^3. \quad (16)$$

For the singlet case we fix, besides $\alpha_s(Q^2) = 0.2$, the input parton densities (9), hence not $F_{2,S}$. The μ_r -dependence of the results for $f = F_{2,S}$, $\dot{F}_{2,\text{NS}} \equiv d \ln F_{2,\text{NS}} / d \ln Q^2$, $\dot{F}_{2,S}$ and $F_{2,S}' \equiv dF_{2,S} / d \ln Q^2$ is presented via

$$\Delta f \equiv \frac{\max \dot{f} - \min \dot{f}}{2 |\text{average } \dot{f}|}, \quad \frac{1}{4} Q^2 \leq \mu_r^2 \leq 4 Q^2. \quad (17)$$

The singlet results are shown for $\mu_f = \mu_r \equiv \mu$.

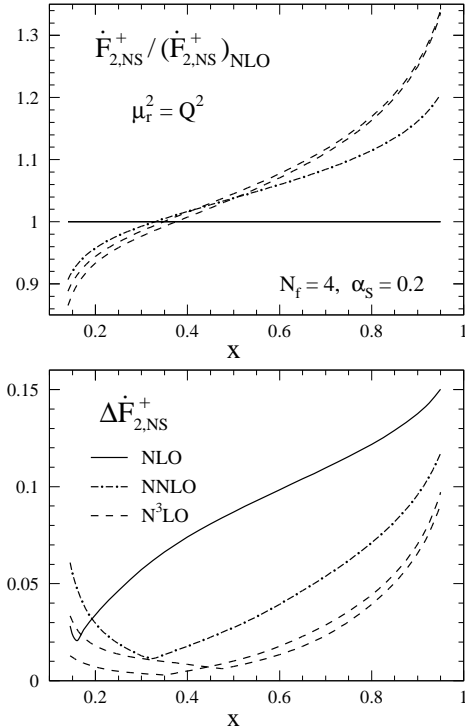


Figure 5. Top: The NNLO and NNNLO corrections for $\dot{F}_{2,\text{NS}}^+$ for the input (15) and (16). Bottom: The relative μ_r -uncertainties (17) compared to the corresponding NLO result.

The results for $\dot{F}_{2,\text{NS}}$ are shown in Fig. 5. The uncertainty bands for the NNNLO predictions take into account both the remaining inaccuracies of the coefficient functions $c_{2,\text{NS}}^{(3)}(x)$ and the possible effects of the splitting functions $P_{\text{NS}}^{(3)}$. At $0.25 \lesssim x \lesssim 0.7$ the μ_r -uncertainties $\Delta \dot{F}_{2,\text{NS}}$ are reduced by a factor of two (four) or more at NNLO (NNNLO). These uncertainties lead to the following estimates for the errors of $\alpha_s(M_Z^2)$ due to the truncation of the perturbation series:

$$\begin{aligned} \Delta \alpha_s(M_Z^2)_{\text{NLO}} &\simeq 0.005 \\ \Delta \alpha_s(M_Z^2)_{\text{NNLO}} &\simeq 0.002 \\ \Delta \alpha_s(M_Z^2)_{\text{NNNLO}} &\simeq 0.001. \end{aligned} \quad (18)$$

A 1% accuracy is achieved at the NNNLO level. As the scaling violations for the same $\alpha_s(Q^2)$ are stronger at NNLO and NNNLO than at NLO, higher-order fits of data on $F_{2,\text{NS}}$ will yield somewhat lower central values of $\alpha_s(M_Z^2)$,

$$\alpha_s(M_Z^2)_{\text{NNNLO}} - \alpha_s(M_Z^2)_{\text{NLO}} \approx -0.002. \quad (19)$$

The results for the singlet case are presented in Fig. 6. $F_{2,S}$ receives large positive corrections at large x , caused by the soft-gluon parts of the quark coefficient functions. The sizeable negative NNLO corrections at small x are dominated by the gluon contribution. It is worth noting that the positive $1/x$ term of $c_{2,g}^{(2)}$ does not dominate this correction even at $x < 10^{-3}$.

The Q^2 -derivative of $F_{2,S}$ is dominated by the quark contribution at $x > 0.3$, and by the gluon contribution at $x < 0.03$. Thus we present the logarithmic derivative $\dot{F}_{2,S}$ in the former x -range, and the linear derivative $F_{2,S}'$ in the latter region. Note that the positive NNLO gluon contribution reaches 5% of the total $|\dot{F}_{2,S}|$ at $x = 0.5$, enough to jeopardize purely non-singlet analyses of F_2^p data also in the region $x > 0.3$.

The reduced μ_r -dependence of both F_2 and its derivatives leads to a better theoretical accuracy of determinations of the parton densities from data on $F_{2,S}$ and $dF_{2,S}/d \ln Q^2$ at $Q^2 \simeq 30 \text{ GeV}^2$: NNLO uncertainties of less than 2% from the truncation of the perturbation series are obtained for the quark density at $10^{-3} < x < 0.5$ and for the gluon density at $3 \cdot 10^{-3} < x < 0.2$.

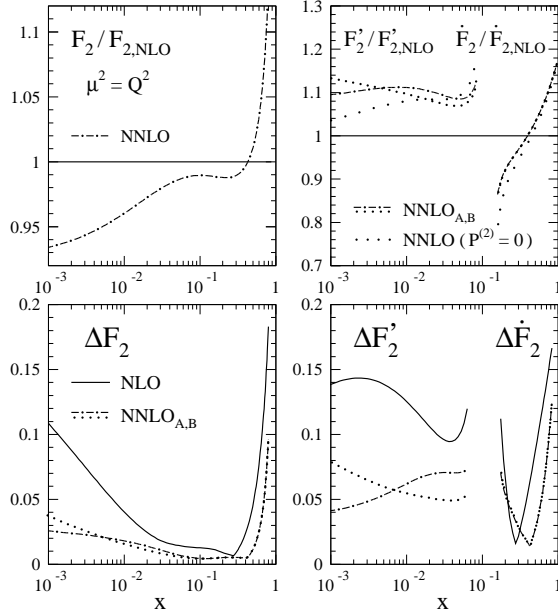


Figure 6. Top: The NNLO corrections for $F_2 \equiv F_{2,S}$ and its Q^2 derivatives for the input (9) at $\mu_{f,0}^2 = Q^2$. Bottom: The corresponding $\mu_r = \mu_f$ uncertainties (17) compared to the NLO results.

8. Summary

We have briefly discussed the evolution of unpolarized parton densities and structure functions in the $\overline{\text{MS}}$ scheme. Our approximate results for the 3-loop splitting functions $P^{(2)}(x)$ pave the way for promoting, even though only at $x > 10^{-3}$, global analyses of DIS and related processes to NNLO accuracy. We will also provide approximations for the 3-loop non-singlet coefficient functions $c_{\text{NS}}^{(3)}$, thus enabling NNNLO determinations of α_s from structure functions at least at $x \geq 0.2$.

At very large x , $x \gtrsim 0.8$, terms even beyond NNNLO are relevant. Here results are available from soft-gluon resummation [17,18]. Progress towards the important HERA small- x region of $x \lesssim 10^{-3}$ at moderate/low Q^2 requires the full calculation of the three-loop splitting functions [14].

FORTAN subroutines of our parametrizations of the 2-loop coefficient functions and our approximations of the 3-loop splitting functions can be obtained from neerven@lorentz.leidenuniv.nl or avogt@lorentz.leidenuniv.nl.

REFERENCES

1. C. Caso et al., Particle Data Group, Eur. Phys. J. **C3** (1998) 1, and references therein
2. W. Furmanski and R. Petronzio, Z. Phys. **C11** (1982) 293, and references therein
3. O.V. Tarasov, A.A. Vladimirov, and A.Yu. Zharkov, Phys. Lett. **B93** (1980) 429; S.A. Larin and J.A.M. Vermaseren, Phys. Lett. **B303** (1993) 334
4. T. van Ritbergen, J.A.M. Vermaseren and S.A. Larin, Phys. Lett. **B400** (1997) 379
5. E.B. Zijlstra and W.L. van Neerven, Phys. Lett. **B272** (1991) 127; *ibid.* **B273** (1991) 476; *ibid.* **B297** (1992) 377
6. E.B. Zijlstra and W.L. van Neerven, Nucl. Phys. **B383** (1992) 525
7. S.A. Larin, T. van Ritbergen, and J.A.M. Vermaseren, Nucl. Phys. **B427** (1994) 41
8. S.A. Larin et al, Nucl. Phys. **B492** (1997) 338
9. J. A. Gracey, Phys. Lett. **B322** (1994) 141
10. J. Blümlein and A. Vogt, Phys. Lett. **B370** (1996) 149
11. J.F. Bennett and J.A. Gracey, Nucl. Phys. **B517** (1998) 241
12. S. Catani and F. Hautmann, Nucl. Phys. **B427** (1994) 475
13. V.S. Fadin and L.N. Lipatov, Phys. Lett. **B429** (1998) 127; and references therein
14. J.A.M. Vermaseren and S. Moch, preprint NIKHEF-00-008 (hep-ph/0004235)
15. W.L. van Neerven and A. Vogt, Nucl. Phys. **B568** (2000) 263
16. W.L. van Neerven and A. Vogt, preprint INLO-PUB 04/00 (hep-ph/0006154).
17. G. Sterman, Nucl. Phys. **B281** (1987) 310; S. Catani and L. Trentadue, Nucl. Phys. **B327** (1989) 323; *ibid.* **B353** (1991) 183
18. A. Vogt, Phys. Lett. **B471** (1999) 97
19. W.L. van Neerven, A. Vogt, in preparation
20. A. Gonzales-Arroyo, C. Lopez and F.J. Yndurain, Nucl. Phys. **B153** (1979) 161
21. J. Blümlein and A. Vogt, Phys. Rev. **D58** (1998) 014020; J. Blümlein et al, Proceedings of DIS 98, Brussels, April 1998, eds. Gh. Coremans and R. Roosen (World Scientific 1998), p. 211 (hep-ph/9806368)
22. A. Retey, J.A.M. Vermaseren, in preparation